Enhanced Hexagonal-Based Search Using Direction-Oriented Inner Search for Motion Estimation

Bei-Ji Zou, Cao Shi, Can-Hui Xu, and Shu Chen

***Abstract*—The newly developed enhanced hexagonal-based search using point-oriented inner search (EHS-POIS) enormously speeds up hexagon-based search (HS). From a different perspective, an inherent correlation between distortion and spatial direction through statistical analysis is found. Based on the observed distortion distribution, a novel enhanced hexagonal-based search with direction-oriented inner search (EHS-DIOS) is proposed to avoid real distortion calculation and thus reduce high computation. Experimental results show that, the proposed algorithm is faster than EHS-POIS by achieving two times improvement in terms of inner search speed, and as compared with previous works, it makes a better tradeoff between speed and decoded image quality.**

***Index Terms*—Directional distortion distribution, hexagon search, inner search, motion estimation.**

I. Introduction

BLOCK matching based motion estimation plays a vital role in video compression, image processing, computer vision, etc. With the aim to find the best matched block in the reference frame, it is natural to utilize full search (FS) comparing all candidate blocks within the search window, which undoubtedly finds the global optimal matched block at cost of high computational complexity. To speed up searching process, many efficient heuristic approaches were proposed successively, such as three-step search (TSS) [1], new three-step search (NTSS) [2], two-dimensional logarithmic search [3], four-step search (FSS) [4] and block-based gradient descent search (BBGDS) [5], etc.

It is well known that the variation of motion vector in real-world image sequences is gentle, smooth, and slow [2], [4]. Experiments [2] also show that the best matched position is always center-biased. This conclusion is well made use of by NTSS, FSS, BBGDS, diamond search (DS) [6], [7], cross-diamond search [8]–[17], hexagon-based search (HS) [9], etc., which are state of the art in motion estimation. In TSS, NTSS, FSS, BBGDS, square-shaped search patterns of different sizes are adopted, while DS employs a diamond-shaped search pattern. To choose different search pattern can result in better performance like diamond-shaped DS outperforming some square-shaped search patterns [1]–[5]. Therefore, Zhu *et al.* further developed a hexagon-shaped search method HS [9], which uses a more circle-approximated search pattern and is more computationally efficient than DS.

Both HS and DS include two search patterns: 1) a coarse search using a relatively large search step to find probable area of global minimal block matching error (BME), and 2) an inner search exploring the small area within the result of the coarse search. Much attention has been given to speed up the coarse search by reducing the number of search points. Actually, the inner search accounts for a non-negligible part of search time. Fast inner search is highly desirable to further reduce search points. Enhanced hexagonal search (EHS) [10] was proposed to improve the inner search speed by saving at least one point from calculating BME against the original HS [9]. By exploiting locally unimodal error surface assumption (LUESA), EHS groups the inner points according to six sides of hexagon, and only checks a portion of inner points with smallest group error. Instead of using such group-oriented method, an enhanced hexagonal-based search using point-oriented search (EHS-POIS) was presented in [11] to optimize the prediction result for each inner point. It is experimentally proved that EHS-POIS outperforms EHS on both accuracy and speed.

The remainder of this letter is organized as follows. In Section II, isoline map is first introduced to illustrate anisotropy of distortion distribution and three new assumptions are made for the proposed inner search strategy. The concept of pseudo-point is developed in Section III, which integrates direction information into a new inner search strategy. In Section IV, the proposed enhanced hexagonal-based search using direction-oriented inner search (EHS-DOIS) is compared with previous works in terms of prediction process computation expense. The experimental results and discussion are presented in Section V, and Section VI concludes this letter.

Manuscript received December 8, 2008; revised March 16, 2009 and May 21, 2009. First version published September 1, 2009; current version published January 7, 2010. This work was supported by the National Natural Science Foundation of China (Project Nos. 60 673 093 and 60 803 024), the Major Program of National Natural Science Foundation of China (Project No. 90715043), the Program for Changjiang Scholars and Innovative Research Team in University (Project No. IRT0661), the Hunan Provincial Natural Science Foundation of China (Project No. 07JJ3125), and the Ph.D. Programs Foundation of Ministry of Education of China (Project No. 200 805 331 107). This paper was recommended by Associate Editor J. F. Arnold.

The authors are with the School of Information Science and Engineering, Central South University, Changsha 410083, China (e-mail: bjzou@vip.163.com; caoshi@yeah.net; christinexu@mail.csu.edu.cn; smallbug2000@163.com).

Color versions of one or more of the figures in this letter are available online at http://ieeexplore.ieee.org.

Digital Object Identifier 10.1109/TCSVT.2009.2031461

II. Anisotropy of Block Matching Error Distribution

As mentioned previously, EHS [10] predicts distortions of grouped inner points by calculating group distortions of hexagon. To optimize the prediction result, EHS-POIS [11] predicts the distortion for each inner point using neighbor points. This inspires us to address a question of particular interest: which neighbor of an inner point should be used for achieving better prediction performance? First take a closer look at the distortion distribution in search window. According to LUESA, the global minimum is always centrally biased. Since error distributions encode important information for prediction of individual inner point, spatial variability of directional anisotropy of error distribution surface is investigated.

Define the average local error surface as matrices

$$E' = \frac{\left(\sum_{k=1}^{N} E_k\right)}{N} \tag{1}$$

$$E'' = \frac{\sum_{f=1}^{M} E'_f}{M} \tag{2}$$

where $E = [\mathrm{SAD}]_{(2W+1)\times(2W+1)}$ is the error matrix including the sum of absolute difference (SAD) between the predefined block and all candidates in the search window with the size of $\pm W$. N is the number of block in a frame, and M is the number of frame in a video. E' and E'' represent the average local error surface in a frame and a video, respectively.

In order to explore anisotropy of BME distribution, the error gradient along directions is exploited to quantify directional dispersion of BME distribution. Let P be a point in the search window. Both the origin of a Cartesian coordinate system and the pole of a polar coordinate system are set on point P. Then the error gradient along a particular direction θ is defined as

$$g_{\theta,i} = \frac{\left[Er(x_{\theta,i}, y_{\theta,i}) - Er(x_{\theta,i-1}, y_{\theta,i-1})\right]}{\Delta\rho_\theta} \tag{3}$$

where θ is the angle in polar coordinates, $(x_{\theta,i}, y_{\theta,i})$ and $(x_{\theta,i-1}, y_{\theta,i-1})$ are Cartesian coordinates of two points along the same direction θ with radius increment $\Delta\rho_\theta$, $i = 1, 2, \ldots, H$, H is the number of explored points along the direction θ, $(x_{\theta,0}, y_{\theta,0})$ is Cartesian coordinates of P, and $Er(x_{\theta,i}, y_{\theta,i})$ is BME of point $(x_{\theta,i}, y_{\theta,i})$. In fact, $x_{\theta,i} = x_{\theta,i-1} + \Delta\rho_\theta \cdot \cos\theta$ and $y_{\theta,i} = y_{\theta,i-1} + \Delta\rho_\theta \cdot \sin\theta$. Hence, the average error gradient along direction θ is defined as

$$g_\theta = \frac{\sum_{i=1}^{H} g_{\theta,i}}{H}. \tag{4}$$

Considering different directions, the mean value and the variance of g_θ can be calculated with (5) and (6)

$$\bar{g} = \frac{\sum_\theta g_\theta}{Z} \tag{5}$$

$$V = \frac{\sum_\theta (g_\theta - \bar{g})^2}{Z} \tag{6}$$

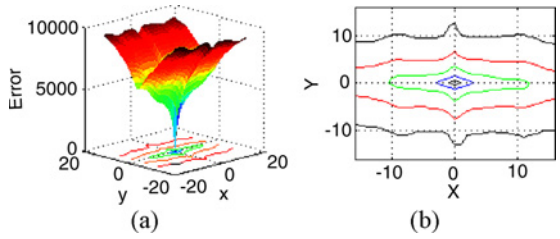

Fig. 1. Directional distribution of distortion in ±16 search window. (a) Error surface for a frame. (b) Isoline map for a frame.

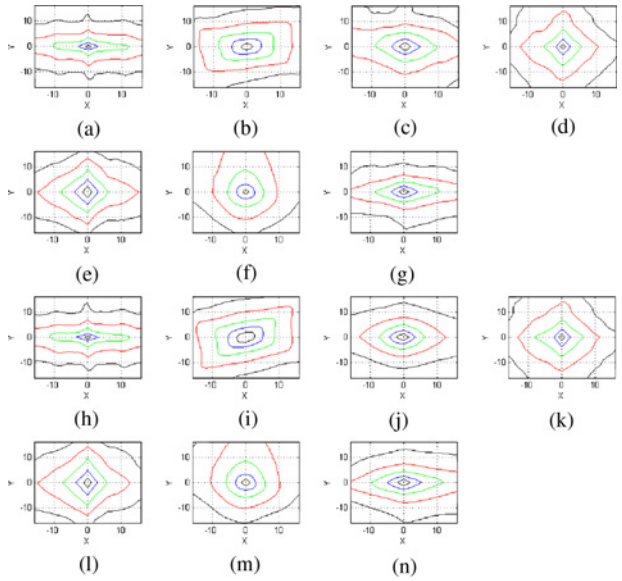

Fig. 2. Error isoline maps of different frames and videos. (a)–(g) Error isoline maps of a singular frame in video *Container*, *Foreman*, *Mobile*, *News*, *Paris*, *Silent*, and *Tempete*, respectively. (h)–(n) Error isoline maps of seven 200-frame videos, respectively.

where Z is the number of different directions investigated. The directional dispersion of BME distribution A can be defined as (7). Generally, higher A indicates stronger anisotropy

$$A = \frac{V}{\bar{g}}. \tag{7}$$

Based on the developed concept, statistical analysis is conducted. The testing set up consists of seven videos (*Container*, *Foreman*, *Mobile*, *News*, *Paris*, *Silent*, and *Tempete*), in which 200 frames per video are used. In each frame, 7×7 nonoverlapping blocks are selected, which are uniformly scattered over the whole image with the same interval along horizontal and vertical lines. The size of block and search window are 16×16 and ± 16, respectively. Therefore, a frame in each video is used for calculating E', and 200 frames are used for E''. The center of search window is chosen as the origin P, and θ is limited to eight directions: $\{0, \pi/4, \pi/2, 3\pi/4, \pi, 5\pi/4, 3\pi/2, 7\pi/4\}$. When $\theta = \pi/4, 3\pi/4, 5\pi/4, 7\pi/4$, $\Delta\rho_\theta = \sqrt{2}$; $\Delta\rho_\theta = 1$, if $\theta = 0, \pi/2, \pi, 3\pi/2$. For (4), H is 16, and the average local error surface E'' is used as Er.

In the video *Container*, the distribution of E' is shown both as surface in Fig. 1(a) and isoline map (contour) in Fig. 1(b). Obviously in 3-D plot of error distribution, a valley along

TABLE I
DIRECTIONAL DISPERSION OF BME DISTRIBUTION

Video	$A = V/\bar{g}$
Container	13.98
Foreman	13.76
Mobile	7.94
News	2.67
Paris	0.91
Silent	8.87
Tempete	10.27

the x-axis is easily spotted. By observing the contour, it is interesting to note that error values are not equally distributed in all directions. To rephrase the fact, the error distribution is not isotropic (i.e., conically symmetric distribution). As Fig. 2 shows, comparing E' and E'', it is amazing distribution shapes for E' and E'' are extremely similar. Hence, BME distribution is undoubtedly anisotropic, and the correlation between BME and spatial direction remains along the time line and is an inherent property in any given video.

Specifically, in Table I and Fig. 2, the error in the videos *Container*, *Foreman*, and *Tempete* increases more slowly along the x-axis. Correspondently, the values of A are relative high. In the videos *News* and *Paris*, error increases uniformly along almost eight directions, so the values of A are low. The nonzero value of A infers that the distribution of BME is correlated with spatial direction. If $A = 0$, the error surface is conical and isolines are circular. Table I quantitively validates the anisotropy of error distribution. It further confirms nonuniformities of each direction's importance for prediction contribution.

Derived from the above statistical analysis, three assumptions are concluded.

1) The distribution of BME is inherently correlated with spatial direction.
2) The correlation between BME and spatial direction is an inherent property along the time line.
3) The assumption that the SAD difference is approximately linearly proportional to the distance (less than two pixels) in [11] is enhanced here. BME is related with not only distance but also direction. BME increases linearly along different directions within two pixels. Error along different directions is nonuniformly distributed.

III. DIRECTION-ORIENTED INNER SEARCH STRATEGY FOR HS

As previously described, the distribution of block matching error is anisotropic to various extent, and eight inner points are inherently around center point of coarse search pattern (CSP), representing eight directions. Consequently, by utilizing the spatial direction information for inner search strategy, the concept of pseudo-points located in eight different directions is introduced to correspond to eight inner points, and then a new direction-oriented inner search scheme is developed for HS.

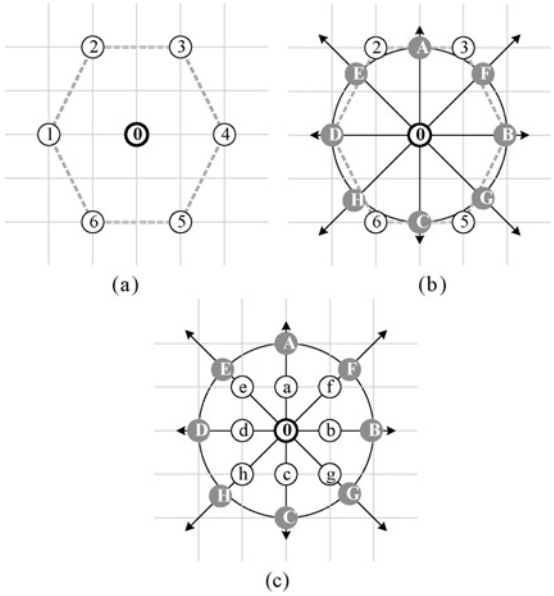

Fig. 3. Novel hexagonal-based search patterns based on direction-oriented inner search. (a) Coarse search pattern (CSP). (b) Pseudo-points prediction pattern (PPPP), in which distortion along eight directions would be predicted through eight pseudo-points: $\{A, B, C, D, E, F, G, H\}$, and eight directions are represented by eight arrows. (c) Inner point prediction pattern (IPPP), in which a point in $\{a, b, c, d, e, f, g, h\}$ would be selected on the arrow from the center of CSP to the pseudo-point with minimal distortion among eight pseudo-points.

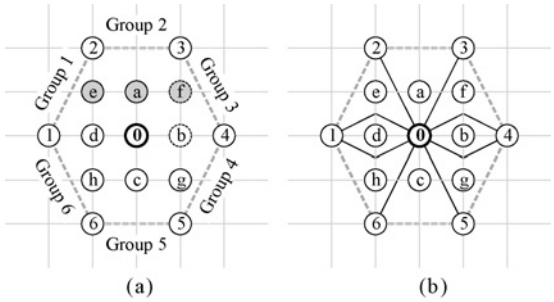

Fig. 4. Prediction Strategies used by EHS and EHS-POIS. (a) Group-oriented prediction of EHS. (b) Point-oriented prediction of EHS-POIS.

It consists of two patterns. The first is called pseudo-points prediction patterns (PPPP). As Fig. 3 shows, eight pseudo-points $\{A, B, C, D, E, F, G, H\}$ are added to the coarse search pattern (CSP) for predicting distortion along eight directions represented by eight arrows. Actually the point "B" and "4" is the same point, so is the point "D" and "1," hence, their BME need not to be calculated. The distortion of other six pseudo-points can be estimated by using the following formula:

$$\sum_{i=1}^{2} \frac{\mathrm{BME}_i}{\sqrt{(x_p - x_i)^2 + (y_p - y_i)^2}} \tag{8}$$

where BME_i represents BME of two nearest points with coordinates(x_i, y_i), $i = 1, 2$, of a particular pseudo-point (x_p, y_p). Taking "A" as an example, the predicted BME of "A" is gained by summing up the normalized BME of two neighbor points "*2*" and "*3*" using formula (8).

The second pattern is named inner point prediction pattern (IPPP). In Fig. 3(c), corresponding to the pseudo-point with minimal distortion among eight pseudo-points, only one point in {*a*, *b*, *c*, *d*, *e*, *f*, *g*, *h*} is selected, and its BME will be calculated and compared with the center point "0" of CSP. The one with smaller BME is the best matching point, e.g., if "*A*" has minimum distortion among eight pseudo-points, the best matching point is the one with min(BME_a, BME_0).

The above proposed algorithm is named enhanced hexagonal-based search using direction-oriented inner search (EHS-DOIS), summarized as follows.

Step 1: The CSP, shown in Fig. 3(a), is located on the center of a search window. If the point with the smallest BME is found to be the center of CSP, proceed to Step 2; otherwise, CSP will shift continually until the smallest BME occurs at the center of CSP.

Step 2: BME of eight pseudo-points, as Fig. 3(b) shows, are predicted through six vertex points in CSP using formula (8). Note that "*B*" and "*D*" need not to be predicted.

Step 3: The corresponding point in {*a*, *b*, *c*, *d*, *e*, *f*, *g*, *h*}, shown in Fig. 3(c), will be selected based on the minimal distortion among BME of eight pseudo-points in Step 2.

Step 4: Calculate the BME of the selected point in Step 3, and comparing it with the center of CSP, the one with smaller BME is the best matching point.

IV. Computation Comparison of Prediction

In this section, the prediction computation expense of concerned algorithms is compared with each other. As shown in Fig. 4(a), EHS [10] groups the six vertexes of the hexagon and accordingly assign eight inner points to candidate group. By comparing the group distortions, it locates the group who is most likely to have inner point with minimal distortion. For example, the sum of distortions of "*2*" and "*3*" are used to predict Group 2 (including inner points "*e*," "*a*," and "*f*"), and the sum of distortions of "*3*" and "*4*" to predict Group 3 (including "*f*" and "*b*"). Hence, in a block matching process, EHS only needs six additions for prediction. By utilizing point-oriented inner search strategy, EHS-POIS [11] predicts the distortion for eight inner points using the "*normalized group distortion* (NGD)" [11] as follows:

$$\mathrm{NGD} = \sum_{i=1}^{N} \frac{\mathrm{SAD}_i}{d_i} = \sum_{i=1}^{N} \frac{\mathrm{SAD}_i}{\sqrt{(x_i - x)^2 + (y_i - y)^2}} \tag{9}$$

where SAD_i represents SAD of two or three nearest points (x_i, y_i) of a particular inner point (x, y). For example, "*0*", "*2*", and "*3*" are used to predict the distortion of "*a*", and "*0*" and "*4*" are used to predict the distortion of "*b*".

It is easy to discover that (8) and (9) are strikingly similar. However the slight difference between is the key to speed up inner search. There are only two neighbors used to predict an individual inner point in (8), but two or mostly three neighbors are used to predict an inner point in (9). In addition, only six pseudo-points need to be calculated for EHS-DOIS, instead, EHS-POIS need to calculate NGD eight times.

The two formulas can be integrated as

$$\sum_{i=1}^{M} \frac{Distortion_i}{Euclidean\,Distance_i}. \tag{10}$$

When it comes to EHS-DOIS, M is definite two. As far as EHS-POIS is concerned, M is two or mostly three. For comparison reason, P-Operation is defined as

$$\frac{Distortion}{Euclidean\,Distance}. \tag{11}$$

The number of operations used by different algorithms is listed in Table II. Obviously, EHS has the lowest computation for prediction, and EHS-DOIS has less computation expense than EHS-POIS in terms of both addition operation and P-Operation.

The prediction computation expense of above algorithms is certainly less than calculating one real distortion. The degree of search speedup mainly depends on the number of checked inner points. Only one inner point needs to be checked by EHS-DOIS constantly. This implies that the proposed inner search theoretically has the faster search ability than previous works.

TABLE II
Operations of a Block Matching Process of Different Algorithms

Operation	EHS	EHS-POIS	EHS-DOIS
Addition	6	14	6
P-Operation	0	22	12

TABLE III
Speed Improvement Rate (%) Over HS

Video	EHS	EHS-POIS	EHS-DOIS
Container	17.11	18.17	27.25
Foreman	14.36	15.90	23.85
Mobile	15.37	16.52	24.77
News	15.10	17.92	26.88
Paris	15.03	17.16	25.73
Silent	15.53	17.40	26.09
Tempete	15.91	16.99	25.48

TABLE IV
Average Psnr Per Frame

Video	HS	EHS	EHS-POIS	EHS-DOIS
Container	33.3370	33.3369	33.3368	33.3368
Foreman	28.4870	27.9503	27.3989	28.0643
Mobile	24.1340	23.9793	24.0089	24.0161
News	31.3509	31.1460	31.1420	31.1485
Paris	28.0350	27.9037	27.9191	27.9256
Silent	31.1725	31.1146	31.1220	31.1422
Tempete	27.6590	27.5830	27.5121	27.5211

V. Experimental Results and Discussion

To evaluate the proposed EHS-DOIS, experiments are conducted to compare HS [9], EHS [10], EHS-POIS [11], and EHS-DOIS in terms of two testing criteria: speed and image quality. For speed comparison, the speed improvement rate (SIR) is introduced: SIR = $(N_{\mathrm{HS}} - N_{\mathrm{Algorithm}})/N_{\mathrm{HS}}$, which reflects the speedup percentage of a particular algorithm relative to HS, where N denotes the total number of points checked by different algorithms. As for image quality, average the peak signal-to-noise ratio (PSNR) per frame is used. HS, EHS, EHS-POIS, and EHS-DOIS are implemented using C++, referring to [14]–[16]. The experiment codes guarantee that none of all algorithms gets any unfair advantage. The setup is as follows: the mentioned seven videos, 106 successive frames per video, block size of 16×16, search window size of ± 16, SAD used.

Note that four algorithms have the same coarse search pattern (CSP), so the number of checked points of CSP is the same. Therefore, the speedup totally depends on the number of checked inner points. From Table III, it is observed that the SIR of EHS, EHS-POIS, and EHS-DOIS is higher than that of HS. The SIR change of EHS-DOIS is around 23.85% to 27.25%, while that of EHS-POIS and EHS are around 15.90% to 18.17% and around 14.36% to 17.11%, respectively, which are significantly lower than that of the proposed algorithm. It is safe to conclude that EHS-DOIS is the fastest one.

From Table IV, in *Container* which contains little motion, EHS-DOIS and EHS-POIS yield 0.002 PSNR decrease compared with HS, and EHS gains 0.001 PSNR increase over the two algorithms. When it comes to *News*, *Paris*, and *Silent*, which contain relatively large motion, EHS-DOIS attains a higher PSNR than both EHS and EHS-POIS. As far as camera panning is concerned, like in *Foreman*, EHS-DOIS yields 0.114 and 0.665 PSNR increase over EHS and EHS-POIS, respectively. When camera zooming and camera panning are both involved in *Mobile* and *Tempete*, EHS-DOIS yields better image quality in some cases. It is obvious that HS yields the highest PSNR in the seven videos. What reason makes HS work so well? Note that HS [9] calculates the real distortions of four inner points "*a*," "*b*," "*c*," "*d*" which distribute along four directions on vertical and horizontal lines. Hence, HS can effectively escape away from a local minimum point. However, EHS-DOIS is able to make the best tradeoff between speed and image quality.

In summary, as far as speed is concerned, EHS-DOIS is undoubtedly the fastest algorithm. In terms of image quality, EHS-DOIS outperforms EHS and EHS-POIS in most cases. The experimental results justify that the proposed direction-oriented inner search is profitable for the hexagon-based search.

VI. Conclusion

In this letter, a new fast inner search was developed to speed up the hexagon search, based on spatial information and anisotropy of error distribution. Isoline map and quantitive analysis on anisotropy were first used to visualize and investigate the error distribution. Three new assumptions about error distribution were concluded for the developed concept of pseudo-point, which integrates direction information into a new inner search strategy. Applying this new strategy, an EHS-DOIS was proposed to speed up HS. Like EHS and EHS-POIS, EHS-DOIS makes its best attempts to reduce the number of checked inner points within hexagon, with its merit of checking only one inner point. Experimental results showed EHS-DOIS gains more speedup than EHS and EHS-POIS, and as compared with previous works, it also outperforms EHS and EHS-POIS in most cases with regard to image quality.

References

[1] T. Koga, K. Iinuma, A. Hirano, Y. Iijima, and T. Ishiguro, "Motion compensated interframe coding for video conferencing ," in *Proc. Nat. Telecommun. Conf.*, New Orleans, LA, Nov.–Dec. 1981, pp. G.5.3.1–G.5.3.5.

[2] R. Li, B. Zeng, and M. L. Liou, "A new three-step search algorithm for block motion estimation," *IEEE Trans. Circuits Syst. Video Technol.*, vol. 4, no. 4, pp. 438–443, Aug. 1994.

[3] J. R. Jain and A. K. Jain, "Displacement measurement and its application in interframe image coding," *IEEE Trans. Commun.*, vol. 29, no. 12, pp. 1799–1808, Dec. 1981.

[4] L. M. Po and W. C. Ma, "A novel four-step search algorithm for fast block motion estimation," *IEEE Trans. Circuits Syst. Video Technol.*, vol. 6, no. 3, pp. 313–317, Jun. 1996.

[5] L. K. Liu and E. Feig, "A block-based gradient descent search algorithm for block motion estimation in video coding," *IEEE Trans. Circuits Syst. Video Technol.*, vol. 6, no. 4, pp. 419–422, Aug. 1996.

[6] J. Y. Tham, S. Ranganath, M. Ranganath, and A. A. Kassim, "A novel unrestricted center-biased diamond search algorithm for block motion estimation," *IEEE Trans. Circuits Syst. Video Technol.*, vol. 8, no. 4, pp. 369–377, Aug. 1998.

[7] S. Zhu and K. K. Ma, "A new diamond search algorithm for fast blockmatching motion estimation," *IEEE Trans. Image Process.*, vol. 9, no. 2, pp. 287–290, Feb. 2000.

[8] C. H. Cheung and L. M. Po, "A novel cross-diamond search algorithm for fast block motion estimation," *IEEE Trans. Circuits Syst. Video Technol.*, vol. 12, no. 12, pp. 1168–1177, Dec. 2002.

[9] C. Zhu, X. Lin, and L. P. Chau, "Hexagon-based search pattern for fast block motion estimation," *IEEE Trans. Circuits Syst. Video Technol.*, vol. 12, no. 5, pp. 349–355, May 2002.

[10] C. Zhu, X. Lin, L. P. Chau, and L. M. Po, "Enhanced hexagonal search for fast block motion estimation," *IEEE Trans. Circuits Syst. Video Technol.*, vol. 14, no. 10, pp. 1210–1214, Oct. 2004.

[11] L. M. Po, C. W. Ting, K. M. Wong, and K. H. Ng, "Novel point-oriented inner searches for fast block motion estimation," *IEEE Trans. on Multimedia*, vol. 9, no. 1, pp. 9–15, Jan. 2007.

[12] B. J. Zou, M. Yang, X. N. Peng, and S. Chen, "A block matching algorithm for motion estimation based on nonbacktracking searching method," *J. Hunan Univ. Natural Sci.*, vol. 35, no. 6, pp. 72–76, Jun. 2008.

[13] B. J. Zou, S. Chen, X. N. Peng, and C. Shi, "Markerless 3-D human motion tracking for monocular video sequences," *J. Comput.-Aided Design Comput. Graphics*, vol. 20, no. 8, pp. 1047–1055, Aug. 2008.

[14] I. E. G. Richardson, "MPEG-4 and H.264 standard," in *H.264 and MPEG-4 Video Compression*. New York: Wiley, 2003, pp. 85–98.

[15] *ITU-T Rec. H.264* [Online]. Available: http://www.itu.int/rec/T-REC-H.264

[16] *JVT H.264/MPEG-4 AVC Reference Software JM10* [Online]. Available: http://iphome.hhi.de/suehring/tml/

[17] C. H. Cheung and L. M. Po, "Novel cross-diamond-hexagonal search algorithms for fast block motion estimation," *IEEE Trans. Multimedia*, vol. 7, no. 1, pp. 16–22, Feb. 2005.

[18] B. J. Zou, S. Chen, C. Shi, U. M. Providence, "Automatic reconstruction of 3-D human motion pose from uncalibrated monocular video sequences based on markerless human motion tracking," *Pattern Recognit.*, vol. 42, no. 7, pp. 1559–1571, Jul. 2009.

[19] K. H. Ng, L. M. Po, K. M. Wong, C. W. Ting, and K. W. Cheung, "A search patterns switching algorithm for block motion estimation," *IEEE Trans. Circuits Syst. Video Technol.*, vol. 19, no. 5, pp. 753–759, May 2009.